Carbohydrate Polymers 104 (2014) 17–22

Contents lists available at ScienceDirect

Carbohydrate Polymers

journal homepage: www.elsevier.com/locate/carbpol

Effect of N-pyridinium positions of quaternized chitosan on transfection efficiency in gene delivery system

Warayuth Sajomsang [a,*], Pattarapond Gonil [a], Uracha Rungsardthong Ruktanonchai [a], Maleenart Petchsangsai [b], Praneet Opanasopit [b], Satit Puttipipatkhachorn [c]

[a] Nanodelivery System Laboratory, National Nanotechnology Center, National Science and Technology Development Agency, Pathum Thani, Thailand
[b] Pharmaceutical Development of Green Innovations Group (PDGIG), Faculty of Pharmacy, Silpakorn University, Nakhon Pathom, Thailand
[c] Department of Manufacturing Pharmacy, Faculty of Pharmacy, Mahidol University, Bangkok, Thailand

ARTICLE INFO

Article history:
Received 31 October 2013
Received in revised form
23 December 2013
Accepted 26 December 2013
Available online 5 January 2014

Keywords:
Chitosan
Quaternized chitosan
N-pyridylmethyl chitosan
Transfection efficiency
Gene delivery

ABSTRACT

Methylated N-pyridylmethyl chitosan chlorides (M-PyMeChCs) with a similar total degree of quaternization (DQ_T) and molecular weight but different N-pyridinium positions were synthesized by reductive amination and methylation, respectively. The effect of N-pyridinium positions on transfection efficiency and cytotoxicity was investigated in human hepatoma (Huh7) cell lines. The results revealed that M-PyMeChCs are able to form a complete complex formation with DNA since there is an *N*/*P* ratio of 5. The particle sizes of M-PyMeChCs/DNA nanopolyplexes were approximately 300 nm and indicated a positive charge. The morphology of these nanopolyplexes was found to be in a spherical shape which was investigated by using the transmission electron microscopy (TEM). The M4-PyMeChC/DNA nanopolyplexes showed highest *in vitro* transfection efficiency in Huh7 cells at *N*/*P* ratio of 20 compared to M2-PyMeChC/DNA and M3-PyMeChC/DNA nanopolyplexes. In comparison to M3-PyMeChC/DNA nanopolyplexes, M2-PyMeChC/DNA and M4-PyMeChC/DNA nanopolyplexes showed lower cytotoxicity in Huh7 cells. Our result demonstrated that N-pyridinium positions of M-PyMeChCs are related to transfection efficiency and cytotoxicity.

1. Introduction

Chitosan (Ch), the cationic (1–4)-2-amino-2-deoxy-β-D-glucan, is industrially produced in various grades, including the medical grade, from chitin of marine origin (Muzzarelli, 2012). Owing to excellent filmogenicity, non-toxicity, and biodegradability, chitosan has been proposed as a safer alternative to other non-viral carriers such as cationic lipids and other cationic polymers (Kim et al., 2007; Muzzarelli, 2010a, 2010b; Weecharangsan, Opanasopit, Ngawhirunpat, Rojanarata, & Apirakaramwong, 2006). However, the limited solubility of chitosan at neutral and basic pH values leads to low transfection efficiency (Kim et al., 2007). On the other hand, quaternized chitosans have excellent solubility over a broader pH range (Germershaus, Mao, Sitterberg, Bakowsky, & Kissel, 2008; Gao, Zhang, Chen, Gu, & Li, 2009; Rojanarata et al., 2008; Safari et al., 2011; Sajomsang, 2010). They are, however, toxic (Kean, Roth, & Thanou, 2005). Instead, among the quaternary ammonium chitosans so far developed for gene delivery, pyridinium derivatives have been shown to be non-toxic for *in vitro* gene delivery (Van Der Woude et al., 1997; Ilies et al., 2004; Pijper et al., 2003) in agreement with our previous report; in fact, we demonstrated that high pyridinium density in nanopolyplexes tended to decrease cytotoxicity due to the delocalization of positive charge into the pyridine ring (Opanasopit et al., 2008; Sajomsang et al., 2013). However, less attention has been paid to the influence of the N-pyridinium positions upon transfection efficiency and cytotoxicity in gene delivery. Therefore, water-soluble chitosan derivatives, namely N-(pyridylmethyl) chitosan chlorides methylated at different pyridine positions 2–4, but similar to each other in the overall degree of quaternization and molecular weight (indicated as M-PyMeChCs), were synthesized and investigated in this study. The effect of N-pyridinium positions of M-PyMeChCs on M-PyMeChCs/DNA ratio, particle size, zeta-potential, morphology, cytotoxicity and transfection efficiency was investigated.

2. Materials and methods

2.1. Materials

The chitosan, which was purchased from Seafresh Chitosan Lab (Bangkok, Thailand), had a molecular weight of 276 kDa

* Corresponding author at: Nanodelivery System Laboratory, National Nanotechnology Center, National Science and Technology Development Agency, Thailand Science Park, Pathum Thani 12120, Thailand. Tel.: +66 2 564 7100x6558; fax: +66 2 564 6981.
E-mail addresses: warayuth@nanotec.or.th, sajomsang@hotmail.com (W. Sajomsang).

0144-8617/$ – see front matter © 2014 Elsevier Ltd. All rights reserved.
http://dx.doi.org/10.1016/j.carbpol.2013.12.077

and 16 kDa and the degree of deacetylation (DDA) at 94% ± 2. Sodium cyanoborohydride and polyethylenimine (PEI) with a molecular weight of 25 kDa were purchased from Aldrich (Milwaukee, USA). Iodomethane, 2-pyridinecarboxaldehyde, 3-pyridinecarboxaldehyde, 4-pyridinecarboxaldehyde, sodium iodide and 1-methyl-2-pyrrolidone (NMP) were sourced from Fluka (Deisenhofen, Germany). 3-(4,5-dimethylthiazol-2-yl)-2,5-diphenyl tetrazolium bromide (MTT) was purchased from Sigma-Chemical Co. (St. Louis, MO, USA). Dulbecco's modified Eagle's medium (DMEM), Trypsin–EDTA, penicillin–streptomycin antibiotics, and fetal bovine serum (FBS) were obtained from GIBCO–Invitrogen (Grand Island, NY, USA). The Human hepatocellular carcinoma (Huh7) cell lines were obtained from the American Type Culture Collection (ATCC, Rockville, MD, USA). All other chemicals were of cell culture and molecular biology grade.

2.2. Synthesis of N-PyMeChs

N-(2-pyridylmethyl) chitosan (2-PyMeCh) was synthesized by reductive amination according to the previously reported procedure (Sajomsang, Rungsardthong Ruktanonchai, Gonil, & Warin, 2010;Sajomsang et al., 2013). Using the same technique described above, 3-pyridinecarboxaldehyde and 4-pyridinecarboxaldehyde were used instead of 2-pyridinecarboxaldehyde. The degree of N-substitution (DS) was determined by ^{1}H NMR spectroscopy (Sajomsang, Tantayanon, Tangpasuthadol, Thatte, & Daly, 2008).

N2-PyMeCh. ATR-FTIR; ν 3283 (O—H and N—H, GlcN), 1592, 1570, 1472 (C=C, aromatic), 1151 (C—O—C, GlcN), 1053, 1020 (C—O, GlcN), and 757 cm^{-1} (C—H, aromatic). ^{1}H NMR (D_2O/CD_3COOD): δ (ppm) 7.2–8.6 (m; 4H Py), 4.4 (br. m; 2H C$\underline{H}_2$—NH) 4.4–3.0 (m, 5H H2–H3), 3.0 (br. s; 1H H2), 1.9 (s; 3H NHAc).

N3-PyMeCh. ATR-FTIR; ν 3282, 1598, 1578, 1475, 1154, 1064, 1020, and 712 cm^{-1}. ^{1}H NMR (D_2O/CD_3COOD): δ (ppm) 7.2–8.5 (m; 4H Py), 4.4 (br. m; 2H C$\underline{H}_2$-NH) 4.4–3.0 (m, 5H H2–H3), 3.0 (br. s; 1H H2), 1.9 (s; 3H NHAc).

N4-PyMeCh. ATR-FTIR; ν 3285, 1605, 1556, 1419, 1149, 1064, 1026, and 793 cm^{-1}. ^{1}H NMR (D_2O/CD_3COOD): δ (ppm) 7.2–6.9 (dd; 4H Py), 4.4 (br. m; 2H C$\underline{H}_2$-NH), 4.4–3.0 (m, 5H H2–H3), 3.0 (br. s; 1H H2), 1.9 (s; 3H NHAc).

2.3. Methylation of N-PyMeChs

Methylation of N2-PyMeCh was carried out according to the previously reported procedure (Sajomsang et al., 2013). A yellow cotton-like M2-PyMeChC powder was obtained. Using the same technique described above, N3-PyMeCh and N4-PyMeCh were used instead of N2-PyMeCh. The degree of quaternization (DQ) was determined by ^{1}H NMR spectroscopy (Sieval et al., 1998).

M2-PyMeChC. ATR-FTIR; ν 3350 (O—H and N—H, GlcN), 1470 (C=C, aromatic), 1469 (C—H, $N^+(CH_3)_3$), 1192 (C—O—C, GlcN), 1098, 1040 (C—O, GlcN), and 800 cm^{-1} (C—H, aromatic). ^{1}H NMR (D_2O): δ (ppm) 8.6–7.5 (dd; 4H Py), 4.6–3.0 (br. m; 26H C$\underline{H}_2$—NH, H2–H6, s, 6H 3, 6-*O*—C$\underline{H}_3$, s; $N^+C\underline{H}_3$ Py, s; 9H $N^+(C\underline{H}_3)_3$), 2.5 (s; 6H $N(C\underline{H}_3)_2$), 2.2 (s; 3H $NC\underline{H}_3$), 1.9 (s; 3H NHAc).

M3-PyMeChC. ATR-FTIR; ν 3380, 1470, 1469, 1192, 1098, 1040, and 843 cm^{-1}. ^{1}H NMR (D_2O): δ (ppm) 8.9–7.8 (dd; 4H Py), 4.6–3.0 (br. m; 26H C$\underline{H}_2$—NH, H2–H6, s, 6H 3, 6-*O*—C$\underline{H}_3$, s; $N^+C\underline{H}_3$ Py, s; 9H $N^+(C\underline{H}_3)_3$), 2.5 (s; 6H $N(C\underline{H}_3)_2$), 2.2 (s; 3H $NC\underline{H}_3$), 1.9 (s; 3H NHAc).

M4-PyMeChC. ATR-FTIR; ν 3347, 1470, 1469, 1192, 1098, 1040, and 845 cm^{-1}. ^{1}H NMR (D_2O): δ (ppm) 8.6–7.9 (dd; 4H Py), 5.1 (br. s; 1H H1′), 4.6–3.0 (br. m; 26H C$\underline{H}_2$—NH, H2–H6, s, 6H 3, 6-*O*—C$\underline{H}_3$, s; $N^+C\underline{H}_3$ Py, s; 9H $N^+(C\underline{H}_3)_3$), 2.5 (s; 6H $N(C\underline{H}_3)_2$), 2.2 (s; 3H $NC\underline{H}_3$), 1.9 (s; 3H NHAc).

2.4. Characterizations

All attenuated total reflectance Fourier transform infrared (ATR-FTIR) spectra were collected with a Nicolet 6700 spectrometer (Thermo Company, USA) using the single-bounce ATR-FTIR spectroscopy (Smart Orbit accessory) with a diamond internal reflection element (IRE) at the ambient temperature (25 °C). The ^{1}H NMR spectra were measured on a Bruker AVANCE 500 MHz spectrometer (Bruker, Switzerland). 1% (v/v) D_2O/CD_3COOD and D_2O were utilized as solvents for 5–10 mg chitosan and its methylated derivatives, respectively. The weight average molecular weight (M_w), number average molecular weight (M_n), and M_w/M_n of chitosan and its methylated derivatives were determined by using the gel permeation chromatography (GPC). The equipment consisted of a Waters 600E Series generic pump, an injector, ultrahydrogel linear columns (M_w resolving range 1 kDa to 20,000 kDa), a guard column, standard pollulans (M_w of 5.9 kDa to 788 kDa), and a refractive index detector (RI). All samples were dissolved in the acetate buffer with a pH of 4 and then filtered through VertiPure 0.45 μm nylon syringes filters (Vertical Chromatography Co., Ltd. Thailand). The mobile phases, 0.5 M AcOH and 0.5 M AcONa (acetate buffer pH 4), were used at a flow rate of 0.6 mL/min at 30 °C. Then an injection volume of 20 μL was used. The *Z*-average hydrodynamic diameter, polydispersity index (PDI) and surface charge of the nanopolyplexes were determined by dynamic light scattering (DLS) using a Zetasizer Nano ZS (Malvern Instruments Ltd., Malvern, UK). All samples were measured at 25 °C in triplicate. The morphologies of nanopolyplexes at optimal *N*/*P* ratios were observed by a transmission electron microscopy (TEM, JEM-100CX II, Japan).

2.5. Preparation of plasmid DNA

The plasmid DNA used was pEGFP-C2 (Clontech, Palo Alto, USA), encoding green fluorescent protein (GFP) which was originally cloned from the mutant *Aequorea victoria*. The pEGFP-C2 was amplified in an *Escherichia coli* DH101 strain according to the previously reported procedure (Sajomsang et al., 2013). The pEGFP-C2 was extracted from the bacterial culture using QIAGEN Hispeed plasmid midi kits (Qiagen, Germany). The purity, concentration and size of plasmid DNA were examined through comparison with the MassRuler DNA ladder mix (Fermentas, USA) for optical densities of 260 and 280 nm and by 1% agarose gel electrophoresis in Tris–boric acid–EDTA (TBE) buffer (BioRad, USA).

2.6. Preparation of nanopolyplexes

The *N*/*P* ratios of nanopolyplexes were calculated by moles of nitrogen atoms in M-PyMeChC and phosphate atoms in DNA. The M-PyMeChC was dissolved in distilled water, followed by an addition of pDNA and incubated for 15 min at room temperature. The *N*/*P* ratios of the nanopolyplexes varied from 0.3 to 20.

2.7. Agarose gel electrophoresis

The binding capacity between M-PyMeChC and pEGFP-C2 was determined by agarose gel electrophoresis at *N*/*P* ratios 0.3–20. The mixtures (10 μL) containing deionized (DI) water, pEGFP-C2, and M-PyMeChC were mixed by pipetting and vortexing, then the nanopolyplexes were allowed to form at room temperature for 15 min. The nanopolyplexes (10 μL) containing 1 μg of pDNA were loaded in each well of 1% agarose gel electrophoresis with a Tris–Boric acid–EDTA (TBE) buffer running 100 V for 40 min. The samples were analyzed under a UV transilluminator (Syngene, UK) after being stained with 1 μg/mL of ethidium bromide.

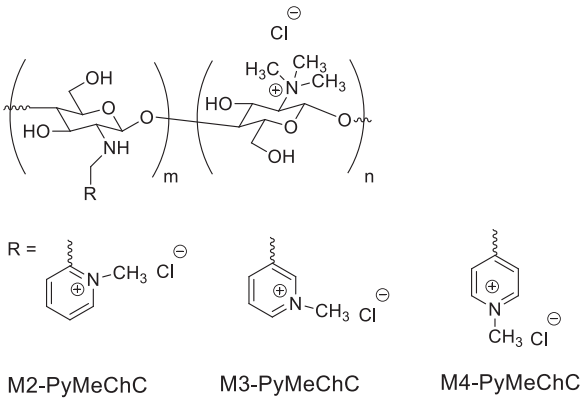

Fig. 1. Chemical structure of methylated N-pyridylmethyl chitosan chloride with different N-pyridinium positions when $m \gg n$.

2.8. In vitro transfection

In vitro transfection studies were performed in Huh7 cells using pEGFP-C2 as a marker gene according to the previously reported procedure (Sajomsang et al., 2013). Non-treated cells, cells transfected with naked plasmid and PEI/DNA nanopolyplexes with a *N*/*P* ratio of 8 were used as controls. After transfection, the cells were washed with PBS twice and grown in a culture medium for 48 h to allow GFP expression. The fluorescent intensity was determined using a flow cytometer (BD Facscalibur™, Germany). All transfection experiments were performed in triplicate.

2.9. Evaluation of cytotoxicity

The evaluation of *in vitro* cytotoxicity was performed by MTT assay according to the previously reported procedure (Sajomsang et al., 2013). Relative viability (%) was calculated based on absorbance at 550 nm using a microplate reader (Universal Microplate Analyzer, Model AOPUS01 and AI53601, Packard BioScience, CT, USA). The viability of non-treated control cells was arbitrarily defined as 100%.

2.10. Statistical analysis

The statistical significance of differences in transfection efficiency and cell viability was examined using one-way analysis of variance (ANOVA) followed by an LSD *post hoc* test. A *p*-value less than 0.05 was considered to be statistically significant.

3. Results and discussion

3.1. Synthesis and characterization of M-PyMeChCs

Water-soluble chitosans, M-PyMeChCs, at different N-pyridinium positions 2–4, but similar to each other in the overall degree of quaternization and molecular weight were carried by reductive amination and quaternization (methylation) of N-PyMeChs, respectively (Sajomsang et al., 2010). Chemical structures of M-PyMeChCs with different N-pyridinium positions are shown in Fig. 1. The degree of N-substitution (DS) was found to range from 72% ± 2 to 80% ± 2 while the total degree of quaternization (DQ_T) was found to range from 77% ± 2 to 85% ± 2 (Table 1). ATR-FTIR and ^{1}H NMR spectroscopy were used to characterize the chemical structures of chitosan and its derivatives, according to our previously reported (Sajomsang et al., 2010, 2013). The ATR-FTIR spectra of the N-PyMeChs were similar to that of chitosan except for the additional absorption bands at wavenumbers 1556–1605, 1556–1570, and 712–793 cm^{-1} due to the C=C stretching and

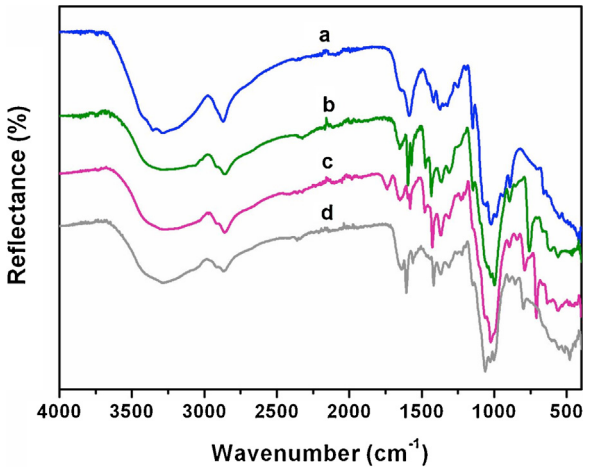

Fig. 2. ATR-FTIR spectra of chitosan (a), N2-pyridyl chitosan (b), N3-pyridyl chitosan (c), and N4-pyridyl chitosan (d).

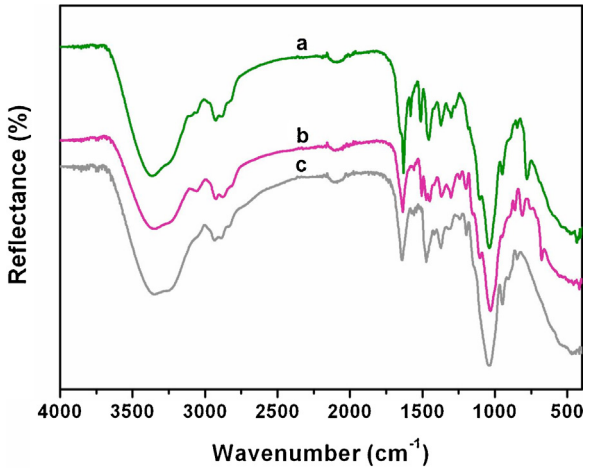

Fig. 3. ATR-FTIR spectra of methylated N2-pyridylmethyl chitosan chloride (a), methylated N3-pyridylmethyl chitosan chloride (b), and methylated N4-pyridylmethyl chitosan chloride (c).

C—H deformation (out of plane) of the pyridyl groups, respectively (Fig. 2). All M-PyMeChCs exhibited the characteristic ATR-FTIR spectra at wavenumber 1470 cm^{-1} due to the C—H symmetric bending of the methyl substituent of quaternary ammonium groups (Fig. 3). The result revealed that the M-PyMeChCs were successfully synthesized.

3.2. Physicochemical characterization of nanopolyplexes

Nanopolyplexes were prepared based on ionotropic gelation technique. The binding capabilities between M-PyMeChCs and DNA were investigated by electrophoresis (Fig. 4). The result revealed that all M-PyMeChCs are able to form complete nanopolyplexes with DNA since the *N*/*P* ratio of 5, and the DNA binding capability is independent on N-pyridinium positions of M-PyMeChCs when similar DQ_T and molecular weight are used. However, the DNA binding capability is dependent on DQ values and molecular weights (Kiang, Wen, Lim, & Leong, 2004; Opanasopit et al., 2008; Sajomsang et al., 2013). The influence of positively charged density and molecular weight on DNA binding capability could be attributed to neutralization and the chain entanglement effect.

The particle size and zeta potential of the nanopolyplexes are investigated at various *N*/*P* ratios, ranging from 0.3 to 20 (Fig. 5). It was found that the particle sizes of all *N*/*P* ratios were

Table 1
Degree of quaternization and molecular weight determination of methylated N-pyridylmethyl chitosans ($n = 3$).

Samples	DS (%)	DQ_T (%)		M_n (kDa)	M_w (kDa)	M_w/M_n	Recovery (%)
		DQ_{py}	DQ_{Ch}				
M2-PyMeChC[a]	78 ± 2	78 ± 2	3 ± 2	5.58	13.26	2.37	70
M3-PyMeChC[a]	80 ± 2	80 ± 2	5 ± 2	3.50	8.44	2.41	75
M4-PyMeChC	72 ± 2	72 ± 2	5 ± 2	5.15	10.05	1.95	63

Recovery (%) = weight of product (g)/weight of starting reactant (g) × 100.
Abbreviations: DS is the degree of N-substitution; DQpy is the degree of quaternization at pyridine substituents; DQCh is the degree of quaternization at primary amino groups of chitosan; DQT is the total degree of quaternization (DQpy + DQCh).
[a] Started from chitosan with M_w = 16 kDa.

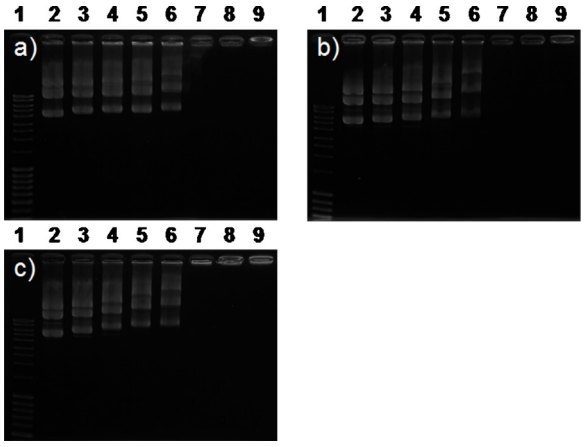

Fig. 4. Gel retardation of nanopolyplexes; methylated N2-pyridylmethyl chitosan chloride (a), methylated N3-pyridylmethyl chitosan chloride (b), and methylated N4-pyridylmethyl chitosan chloride (c). Lane 1, DNA marker and lane 2 DNA; lanes 3–9, nanopolyplexes at *N*/*P* ratios of 0.3, 0.5, 1, 3, 5, 10, and 20, respectively.

approximately 300 nm, indicating that there is no significant effect of molecular weight ranging from 8 to 13 kDa on particle sizes. The zeta potentials of the nanopolyplexes rose with an increase in *N*/*P* ratios. This is due to the highly negative charge of the DNA, which was rapidly neutralized, and then the surface charge of the nanopolyplexes changed to positive values at higher *N*/*P* ratios. The morphologies of nanopolyplexes at a *N*/*P* ratio of 5 were investigated by TEM (Fig. 6). M4-PyMeChC/DNA nanopolyplexes showed a rather spherical shape compared to other nanopolyplexes.

3.3. *In vitro transfection efficiency*

In this study, the effect of N-pyridinium positions of M-PyMeChCs on transfection efficiency was investigated. *In vitro* transfection experiments were performed by evaluating GFP expression of all nanopolyplexes at *N*/*P* ratios between 0.3 and 20 on the Huh7 cells (Fig. 7). Naked DNA was used as a negative control, while branched PEI (25 kDa) at an optimized *N*/*P* ratio of 8 was used as a positive control. As shown in Fig. 7, the transfection efficiencies of nanopolyplexes in Huh7 cells depended on the *N*/*P* ratios and N-pyridinium positions of M-PyMeChCs. In our previous report, we found that the transfection efficiency of M4-PyMeChCs was dependent on the DQ_{ST} (Opanasopit et al., 2008). The transfection efficiency increased with an increasing DQ_T. However, this factor might be dependent on the type of cell lines and the cytotoxicity of the quaternized chitosan derivatives. Moreover, we found that molecular weights of M3-PyMeChCs were affected on transfection efficiency. At similar DQ_{ST}, the M3-PyMeChC with a molecular weight of 82 kDa showed highest transfection efficiency in Huh7 cells compared to molecular weights of 56 and 8 kDa (Sajomsang et al., 2013). The effect of the molecular weight of the chitosan on transfection efficiency can be described by the chain entanglement effect (Kiang et al., 2004). The high molecular weight of chitosan is more easily entangled with free DNA once the initial electrostatic interaction has occurred, leading to the formation of compact nanopolyplexes. It is important to note that transfection efficiency is also dependent on pyridinium/trimethyl ammonium (Py/Tr) ratios of M3-PyMeChC nanopolyplexes at similar DQ_{ST} (Sajomsang et al., 2013). The effect of Py/Tr ratio on transfection efficiency can be explained in terms of the hydrophobic effect (Kurisawa, Yokoyama, & Okano, 2000). Besides *N*/*P* ratios, DQ_{ST}, molecular weights, and Py/Tr ratios, polymer architectures are also affected by transfection efficiency (Liu & Reineke, 2007; Sajomsang, Ruktanonchai, Gonil, Mayen, & Opanasopit, 2009). Previously, we found that transfection efficiency is dependent on chemical structures of quaternary ammonium moieties substituted on the chitosan backbone. The rank of transfection efficiency of nanopolyplexes on Huh 7 cells was found to be M4-PyMeChC > methylated N-(4-N,N-dimethylaminobenzyl) chitosan chloride (MDMBzChC) > trimethyl chitosan chloride (TMChC) > methylated N-(4-N,N-dimethylaminocinnamyl) chitosan chloride (MDMCMChC), respectively. It is possible that the positive charge in the pyridine ring enhance transfection efficiency compared to other quaternized hydrophobic chitosan derivatives (Sajomsang, 2010). Here, we demonstrated that M4-PyMeChC

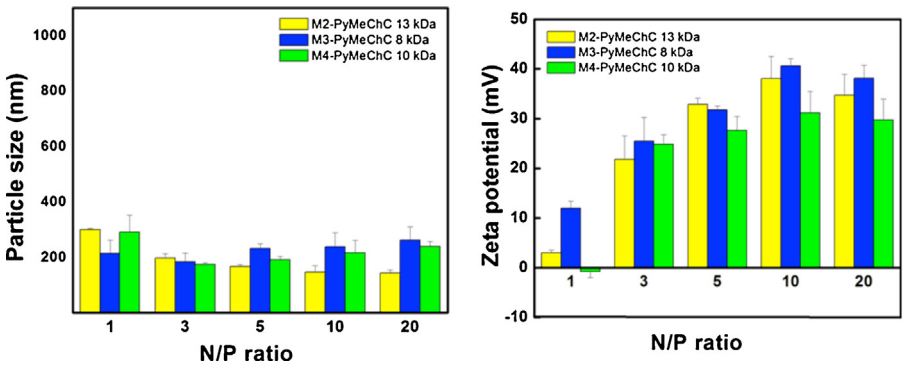

Fig. 5. The particle sizes and zeta potentials of nanopolyplexes with different N-pyridinium positions.

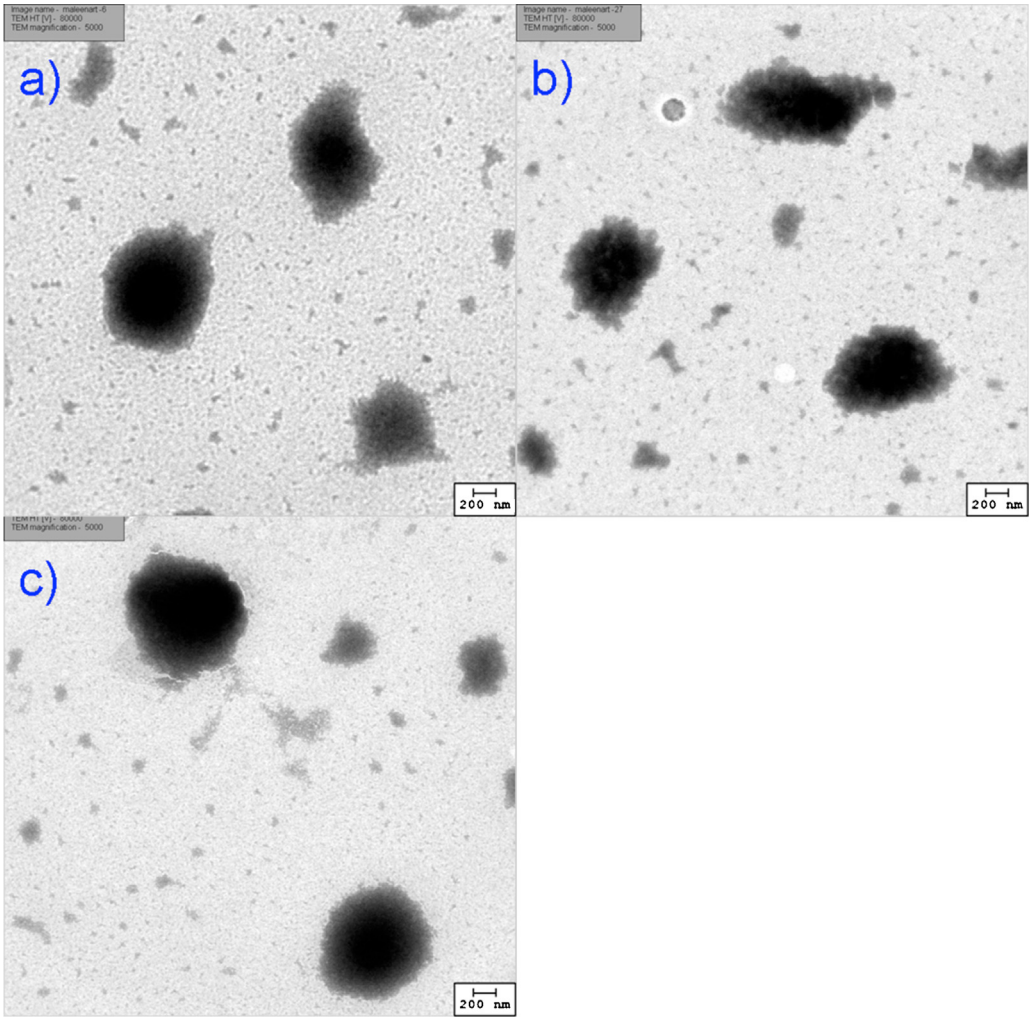

Fig. 6. TEM images of nanopolyplexes with different N-pyridinium positions; methylated N2-(pyridylmethyl) chitosan chloride (a), methylated N3-(pyridylmethyl) chitosan chloride (b), and methylated N4-(pyridylmethyl) chitosan chloride (c).

showed better transfection efficiency than M2-PyMeChC and M3-PyMeChC in Huh 7 cells at *N*/*P* ratio 20 with similar DQ_T and molecular weight.

3.4. Evaluation of cytotoxicity

The cytotoxicity of nanopolyplexes was investigated in Huh7 cells by MTT assay. In this study, PEI/DNA nanopolyplex was used as the control. The results revealed that cytotoxicity of nanopolyplexes was related to the *N*/*P* ratios and N-pyridinium positions of M-PyMeChCs (Fig. 8). The cytotoxicity of nanopolyplexes rose significantly with increasing the *N*/*P* ratios, particularly M3-PyMeChCs/DNA nanopolyplexes, while M2-PyMeChCs/DNA and M4-PyMeChCs/DNA nanopolyplexes showed lower cytotoxicity even though the *N*/*P* ratios were increased. We expected that if DQ_T values and molecular weights of M-PyMeChCs are similar, therefore, the N-pyridinium positions of M-PyMeChCs may relate to cytotoxicity. It is possible that the difference in cytotoxicity of M2-PyMeChC/DNA, M3-PyMeChC/DNA and M4-PyMeChC/DNA nanopolyplexes was due to the N-pyridinium positions of the M-PyMeChCs and the positively charged location. Delocalization of the positive charge in N-pyridinium group at 2 and 4 positions of nitrogen atom are preferred compared to 3 positions of nitrogen atom, leading to a reduction in cytotoxicity. In our study, we demonstrated that at an *N*/*P* ratio of 20, the M4-PyMeChC/DNA

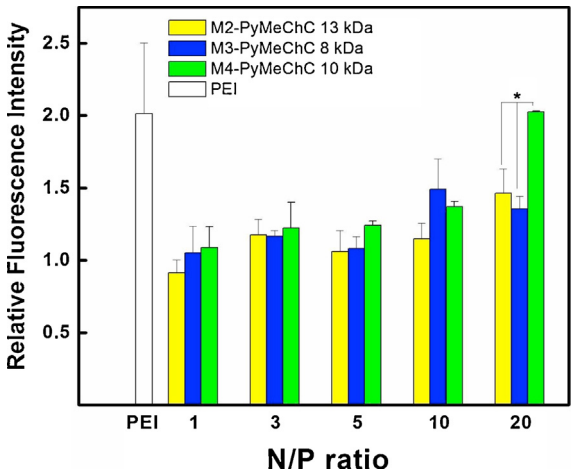

Fig. 7. *In vitro* transfection efficiencies of nanopolyplexes with different N-pyridinium positions in Huh7 cells. Branched PEI (M_w 25 kDa) was used as a control. $^*p < 0.05$ when nanopolyplexes methylated N4-(pyridylmethyl) chitosan chloride compared to nanopolyplexes methylated N3-(pyridylmethyl) chitosan chloride and methylated N2-(pyridylmethyl) chitosan chloride. Data are represented as mean ± standard deviation ($n = 3$).

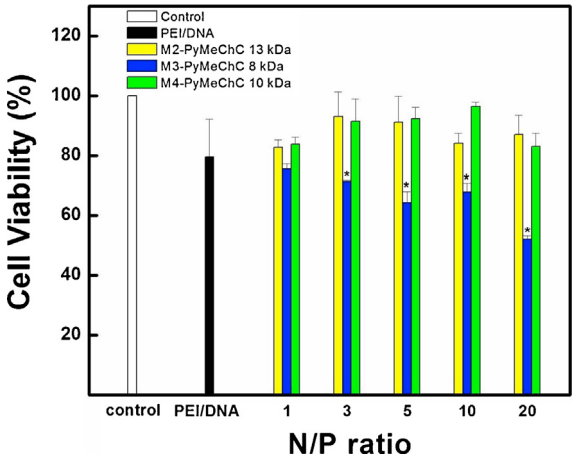

Fig. 8. *In vitro* cytotoxicity of nanopolyplexes with different N-pyridinium positions in Huh7 cells. $^{*}p < 0.05$ when nanopolyplexes methylated N3-(pyridylmethyl) chitosan chloride compared to nanopolyplexes methylated N2-(pyridylmethyl) chitosan chloride and methylated N4-(pyridylmethyl) chitosan chloride. Data are represented as mean ± standard deviation ($n = 3$).

nanopolyplexes showed the highest *in vitro* transfection with 80% cell viability.

4. Conclusion

We demonstrated that N-pyridinium positions of M-PyMeChCs were affected on transfection efficiency and cytotoxicity when DQ_T values and molecular weights were similarly. The M4-PyMeChC showed highest transfection efficiency at a *N*/*P* ratio of 20 compared to M2-PyMeChC and M3-PyMeChC. In comparison to M3-PyMeChC, M2-PyMeChC and M4-PyMeChC showed lower cytotoxicity at all *N*/*P* ratios. Our results indicated that the N-pyridinium positions of the M-PyMeChCs play an important role in transfection efficiency and cytotoxicity.

Acknowledgments

We gratefully acknowledge financial support from the Research, Development and Engineering (RD&E) Fund through the National Nanotechnology Center (NANOTEC), National Science and Technology Development Agency (NSTDA), Thailand (Project No. NN-B-22-EN4-94-51-10).

References

Gao, Y., Zhang, Z., Chen, L., Gu, W., & Li, Y. (2009). Chitosan N-betainates/DNA self-assembly nanoparticles for gene delivery: In vitro uptake and transfection efficiency. *International Journal of Pharmaceutics*, *371*, 156–162.

Germershaus, O., Mao, S., Sitterberg, J., Bakowsky, U., & Kissel, T. (2008). Gene delivery using chitosan, trimethyl chitosan or polyethyleneglycol-graft-trimethyl chitosan block copolymers: Establishment of structure–activity relationships in vitro. *Journal of Controlled Release*, *125*, 145–154.

Ilies, M. A., Seitz, W. A., Ghiviriga, I., Johnson, B. H., Miller, A., Thompson, E. B., et al. (2004). Pyridinium cationic lipids in gene delivery: A structure–activity correlation study. *Journal of Medicinal Chemistry*, *47*, 3744–3754.

Kean, T., Roth, S., & Thanou, M. (2005). Trimethylated chitosans as non-viral gene delivery vectors: Cytotoxicity and transfection efficiency. *Journal of Controlled Release*, *103*, 643–653.

Kiang, T., Wen, J., Lim, H. W., & Leong, K. W. (2004). The effect of the degree of chitosan deacetylation on the efficiency of gene transfection. *Biomaterials*, *25*, 5293–5301.

Kim, T. H., Jiang, H. L., Jere, D., Park, I. K., Cho, M. H., Nah, J. W., et al. (2007). Chemical modification of chitosan as a gene carrier in vitro and in vivo. *Progress in Polymer Science*, *32*, 726–753.

Kurisawa, M., Yokoyama, M., & Okano, T. (2000). Transfection efficiency increases by incorporating hydrophobic monomer units into polymeric gene carriers. *Journal of Controlled Release*, *68*, 1–8.

Liu, Y., & Reineke, T. M. (2007). Poly(glycoamidoamine)s for gene delivery: Structural effects on cellular internalization, buffering capacity, and gene expression. *Bioconjugate Chemistry*, *18*, 19–30.

Muzzarelli, R. A. A. (2010a). Chitosans: New vectors for gene therapy. In R. Ito, & Y. Matsuo (Eds.), *Handbook of carbohydrate polymers: Development, properties and applications* (pp. 583–604). Hauppauge NY, USA: Nova Publ.

Muzzarelli, R. A. A. (2010b). Chitins and chitosans as immunoadjuvants and non-allergenic drug carriers. *Marine Drugs*, *8*(2), 292–312.

Muzzarelli, R. A. A. (2012). Nanochitins and nanochitosans, paving the way to eco-friendly and energy-saving exploitation of marine resources. *Polymer Science: A Comprehensive Reference*, *10*, 153–164.

Opanasopit, P., Sajomsang, W., Ruktanonchai, U., Mayen, V., Rojanarata, T., & Ngawhirunpat, T. (2008). Methylated *N*-(4-pyridinylmethyl) chitosan as a novel effective safe gene carrier. *International Journal of Pharmaceutics*, *364*, 127–134.

Pijper, D., Bulten, E., Šmisterová, J., Wagenaar, A., Hoekstra, D., Engberts, J. B. F. N., et al. (2003). Novel biodegradable pyridinium amphiphiles for gene delivery. *European Journal of Organic Chemistry*, *22*, 4406–4412.

Rojanarata, T., Petchsangsai, M., Opanasopit, P., Ngawhirunpat, T., Ruktanonchai, U., Sajomsang, W., et al. (2008). Methylated N-(4-N,N-dimethylaminobenzyl) chitosan for novel effective gene carriers. *European Journal of Pharmaceutics and Biopharmaceutics*, *70*, 207–214.

Safari, S., Dorkoosha, F. A., Soleimani, M., Zarrintan, M. H., Akbari, H., Larijani, B., et al. (2011). N-Diethylmethyl chitosan for gene delivery to pancreatic cancer cells and the relation between charge ratio and biologic properties of polyplexes via interpolations polynomial. *International Journal of Pharmaceutics*, *420*, 350–357.

Sajomsang, W. (2010). Synthetic methods and applications of chitosan containing pyridylmethyl moiety and its quaternized derivatives: A review. *Carbohydrate Polymers*, *80*, 631–647.

Sajomsang, W., Tantayanon, S., Tangpasuthadol, V., Thatte, M., & Daly, W. H. (2008). Synthesis and characterization of N-aryl chitosan derivatives. *International Journal of Biological Macromolecules*, *43*, 79–87.

Sajomsang, W., Ruktanonchai, U., Gonil, P., Mayen, V., & Opanasopit, P. (2009). Methylated *N*-aryl chitosan derivative/DNA complex nanoparticles for gene delivery: Synthesis and structure–activity relationships. *Carbohydrate Polymers*, *78*, 743–752.

Sajomsang, W., Rungsardthong Ruktanonchai, U., Gonil, P., & Warin, C. (2010). Quaternization of *N*-(3-pyridylmethyl) chitosan derivatives: Effects of the degree of quaternization, molecular weight and ratio of *N*-methylpyridinium and *NNN*-trimethyl ammonium moieties on bactericidal activity. *Carbohydrate Polymers*, *82*, 1143–1152.

Sajomsang, W., Gonil, P., Ruktanonchai, U., Petchsangsai, M., Opanasopit, P., & Puttipipatkhachorn, S. (2013). Effects of molecular weight and pyridinium moiety on water-soluble chitosan derivatives for mediated gene delivery. *Carbohydrate Polymers*, *91*, 508–517.

Sieval, A. B., Thanou, M., Kotze, A. F., Verhoef, J. C., Brussee, J., & Junginger, H. E. (1998). Preparation and NMR characterization of highly substituted trimethyl chitosan chloride. *Carbohydrate Polymers*, *36*, 157–165.

Van Der Woude, I., Wagenaar, A., Meekel, A. A. P., Ter Beest, M. B. A., Ruiters, M. H. J., Engberts, J. B. F. N., et al. (1997). Novel pyridinium surfactants for efficient, nontoxic in vitro gene delivery. *Proceedings of the National Academy of Sciences of the United States of America*, *94*, 1160–1165.

Weecharangsan, W., Opanasopit, P., Ngawhirunpat, T., Rojanarata, T., & Apirakaramwong, A. (2006). Chitosan lactate as a nonviral gene delivery vector in COS-1 cells. *American Association Pharmaceutical Scientists PharmSciTech*, *7*, E74–E79.